AIAA JOURNAL
Vol. 30, No. 8, August 1992

Gas-Particle Nonequilibrium Nozzle Flows: Concept of Virtual Speed of Sound and Similar Solutions

R. K. Thulasiram* and N. M. Reddy†
Indian Institute of Science, Bangalore, India

An attempt is made to obtain similar solutions for gas-particle nonequilibrium nozzle flows. Modified definitions for speed of sound and Mach number are proposed for this study. The governing equations are transformed into a similar form and a single correlating parameter is obtained. The limiting (equilibrium and frozen) speeds of sound are shown to be derivable from the modified definition. The numerical results transpire several interesting phenomena occurring in the nozzle. For example, the approach to isothermal condition of the flow at very large loading ratio is proved with no assumption regarding the lag of the particles. By varying the numerical values of the general correlating parameter, the complete nonequilibrium regime of the flow can be scanned. With the present similar solutions, the flow quantities in a nozzle can be readily determined for different particle sizes, loading ratios, reservoir conditions, and for a family of nozzle shapes without resorting to complex computer programs.

Nomenclature

A, A_v = geometric and virtual area ratio of the nozzle
a = speed of sound
a_e, a_f = equilibrium and frozen speeds of sound in gas-particle mixture
a_v = virtual speed of sound in gas-particle mixture
C_D = viscous drag coefficient of the particles
c = specific heat of the particle material
c_v, c_p = specific heat of the gas phase at constant volume and pressure
d_p = diameter of the (spherical) particles
i, j = nozzle shape parameters
K = velocity ratio introduced in Eq. (4), u_p/u
L' = nozzle scale parameter defined as $r'_*/\tan\theta$
M = Mach number
M_v = virtual Mach number in gas-particle mixture
$\dot{m}$, $\dot{m}_p$ = mass flow rate of gas and particles
N_s = function introduced in Eqs. (26) and (27)
p = pressure
R = gas constant
Re = Reynolds number (based on particle diameter)
r = nozzle throat radius
S_0, S_r = reservoir and reference entropy
T, T_p = temperatures of gas and particle phases
u, u_p = velocities of gas and particle phases
x = distance along the nozzle axis
Z = parameter introduced in Eq. (4), $1 + \eta K$
α = independent variable introduced for transformation
γ, Γ = specific heat ratio of the gas phase and gas-particle mixture
δ = relative specific heat of the particles and gas, c/c_p
ζ, ω = volume and mass fraction of the particle phase in the mixture
η = loading ratio, $\dot{m}_p/\dot{m}$
θ = angle of inclination of the nozzle wall from the axis
λ = parameter introduced in Eqs. (26) and (27)
μ = viscosity of the gas phase
ξ = independent variable introduced in Eq. (32)
ρ, ρ_p = density of gas and particle phases
σ,σ_p = concentration of gas and particle phases in the mixture
τ_v = velocity relaxation time of particles, $\rho_p d_p^2/18\mu$
χ = general correlating parameter

Subscripts

p = pertaining to particles
0, * = reservoir and nozzle throat conditions

Superscript

= dimensional quantities

Introduction

FOR the past several years, metallized propellants in solid rocket motors have been used to stabilize combustion as well as to attain larger specific impulse. Since the propellant is burned in the combustion chamber, the metal additives of the propellants get oxidized and come out as metal oxide particles. These products of combustion have increased the interest in estimating phase nonequilibrium effects on the nozzle flow performance. As the condensed combustion products can do no work, their presence in the nozzle could only be deleterious to the effectiveness of the nozzle expansion process. The particle products of combustion are accelerated almost exclusively by the drag or slippage of the particles relative to the expanding gas, and the gas loses a part of its energy in accelerating the particles. There are several studies[1-7] on gas-particle flows reported in the literature employing analytical and numerical techniques for analyzing the flow phenomena in a nozzle. References 8 and 9 present the fundamentals of the two-phase flows. A near-exhaustive review of the literature is presented in Ref. 10.

Nozzle flows of gases with a large number of particles (i.e., η is large) are of interest in injection of metallic fuel powder into rocket engine combustion chambers, nuclear reactors, chemical industries for conveying particulate materials, and many other engineering applications. Some aspects of the gas-particle nozzle flow when the particles occupy a finite volume in the mixture are reported in Refs. 11 and 12. In most of the applications, the choice of whether to neglect the particle volume (in the mixture) or not is dictated by the practical situation. Some practical situations in which the particle volume fraction cannot be neglected are 1) when the mass fraction of the particles ω is very high and 2) when the particle

Received May 9, 1991; revision received Nov. 15, 1991; accepted for publication Dec. 4, 1991.

*Research Scholar; currently Post-Doctoral Fellow, Department of Mechanical Engineering, Concordia University, Montreal H3G 1M8, Canada. Member AIAA.

†Professor, Department of Aerospace Engineering. Associate Fellow AIAA.

material density ρ_p' is small so that the density ratio of the gas to that of the particle material ρ'/ρ_p' will be greater than 10^{-3}.

In case the particle loading is high, which leads to a condition that the particle volume fraction in the mixture cannot be ignored, the particle volume fraction itself becomes a variable and further complicates the analysis. Hence, solving the governing equations for this kind of two-phase flow problems becomes difficult.

Scope and Purpose of the Present Work

In all of the studies on gas-particle nozzle flows, the analysis is based on the frozen speed of sound. A recent study[7] on the physical aspects of the relaxation model in two-phase flow also presents the analysis with two limiting velocities of wave propagation. However, in many of the practical situations, the gas-particle flow involved is of a nonequilibrium nature, and the very presence of the particles in the flow affects the wave propagation in the mixture.

There seems to be no precise definition for speed of sound in gas-particle flows taking into account the phase nonequilibrium effects. Consequently, the Mach number-velocity-area ratio relation for the nonequilibrium case does not exist at present. The currently available equilibrium or frozen speed of sound can be used only as limiting cases. Because of the very fact that the particles present in practical situations are neither of submicron range to lead the flow to equilibrium condition nor of very high dimensions to make themselves frozen at their initial conditions, one has to treat the nozzle flow to be in the nonequilibrium regime. In such cases, use of the two limiting definitions of speed of sound turn out to be an approximation. Therefore, it becomes necessary that the definition of speed of sound in nonequilibrium regime of gas-particle nozzle flow be modified.

Moreover, analysis of the gas-particle nozzle flow is made complex because many parameters are required to specify the particle characteristics in addition to the parameters specifying the gas characteristics and nozzle shape. The present state of the art for analyzing nonequilibrium gas-particle nozzle flows requires complex computer programs with which flow variables are determined by numerical integration for given parametric conditions. These usually are the reservoir conditions, nozzle shape, and a specified gas. The computational procedure has to be repeated at different conditions to study the effect on the nozzle flow performance, regardless of the numerical method used. Therefore, if all of the parameters can be combined into a correlating parameter, a single value of which will represent several combinations of the parametric conditions of the problem, the cumbersome job of repeating the solution procedure can be obviated.

The main concern here is on the nonequilibrium effects in one-dimensional gas-particle nozzle flows wherein the particles occupy a finite volume in the mixture. The gas is assumed to be a perfect gas and internal energy nonequilibrium of the gas is not considered. By a suitable modification of the definition of speed of sound, new expressions relating Mach number, velocity, and area ratio are obtained. Then, following the basic methodology reported[13,14] earlier, the governing equations have been transformed into a similar form and a general correlating parameter has been obtained. The results obtained by solving these similar equations numerically are presented in the form of graphs and discussed.

Concept of Virtual Speed of Sound

One of the important physical quantities in the study of gas-particle flows is the speed of sound. For a pure perfect gas, it is given by $a^2 = (\partial p/\partial \rho)_s = \gamma RT$. The expressions for the limiting (equilibrium and frozen) speeds of sound are available[8,9] in the literature for gas-particle flows. As mentioned earlier, practical situations dictate the use of particle sizes of moderate ranges for any theoretical study. Once the particle sizes are in such a way that neither of the two limits of speed of sound could be used, a need for a general expression for the speed of sound is felt.

The gas-particle nozzle flow problem generally contains two sets of equations, one for each phase. For the steady one-dimensional adiabatic case, it is usual to write them in a combined form. The mass and momentum equations are given by

Continuity (gas):

$$\sigma u A = \dot{m} = \text{const} \tag{1}$$

Continuity (particles):

$$\sigma_p u_p A = \dot{m}_p = \eta \dot{m} = \text{const}$$

Momentum (mixture):

$$\sigma u \frac{du}{dx} + \sigma_p u_p \frac{du_p}{dx} + \frac{dp}{dx} = 0 \tag{2}$$

or

$$\sigma u \frac{du}{dx} + \eta \sigma u \frac{du_p}{dx} + \frac{dp}{dx} = 0 \tag{3}$$

The nonequilibrium nature of the gas-particle flow and the ratio of the mass flow rates (loading ratio) can be effectively

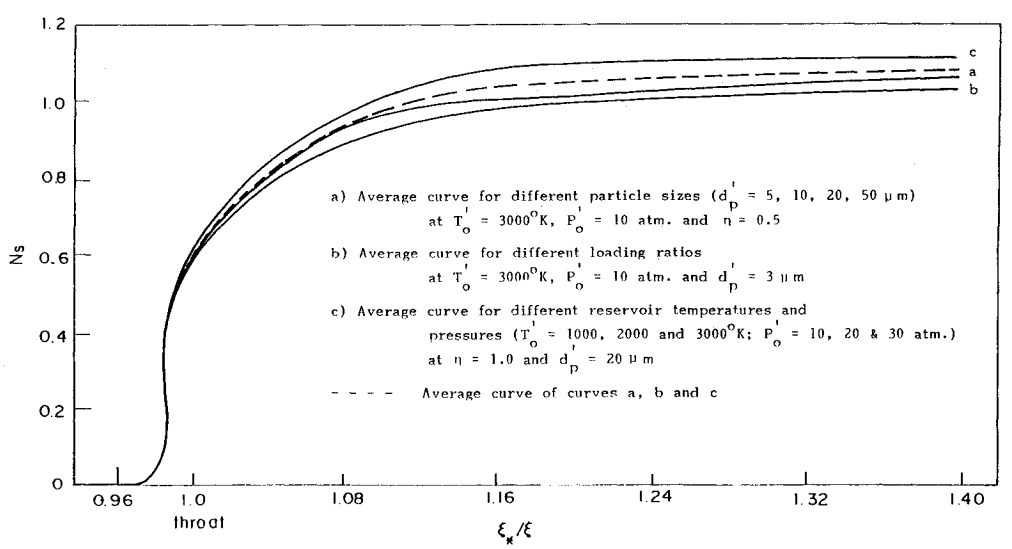

Fig. 1 Mean curves and a single correlation for N_s.

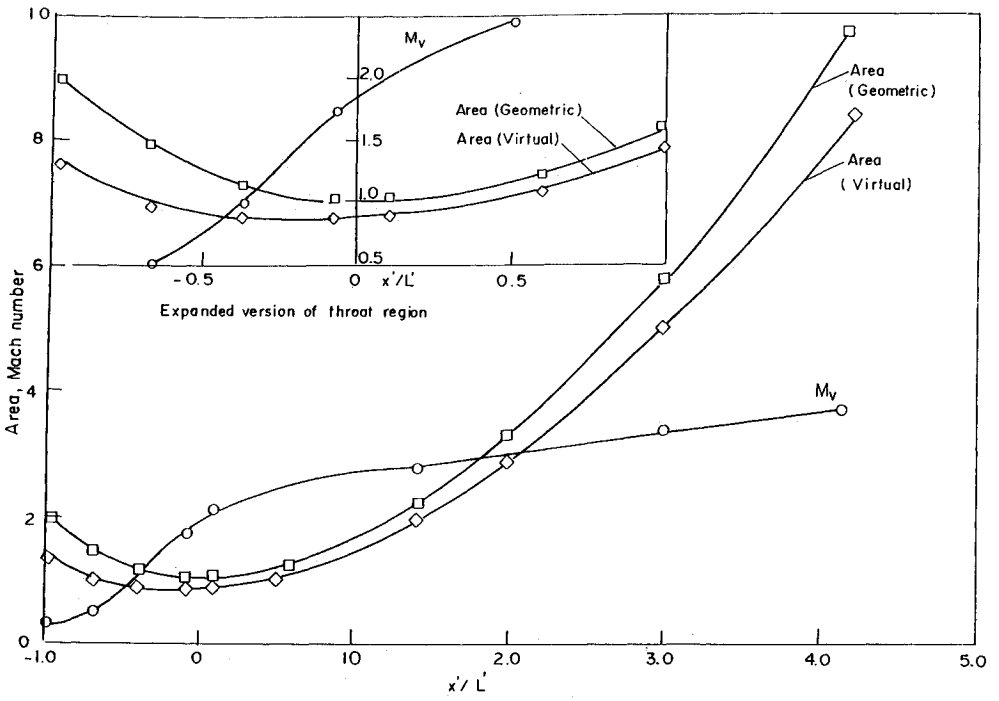

Fig. 2 Variation of virtual area and virtual Mach number along the nozzle axis.

introduced[15] by a parameter $Z = (1 + \eta u_p/u)$; Z can also be written as

$$Z = (1 + \eta K) \tag{4}$$

where $K = u_p/u$. Also, this expression for Z can be written in the differential form as

$$\mathrm{d}[\ell n(u_p)] = \mathrm{d}[\ell n(u)] + \mathrm{d}[\ell n(Z - 1)] \tag{5}$$

From the definition of K results

$$\mathrm{d}u_p = Ku\ \mathrm{d}[\ell n(K)] + Ku\ \mathrm{d}[\ell n(u)] \tag{6}$$

From the continuity equation

$$\mathrm{d}u = -u\ \mathrm{d}[\ell n(\sigma)] - u\ \mathrm{d}[\ell n(A)] \tag{7}$$

Using Eqs. (6) and (7), the momentum equation (2) can be written as

$$-\{\mathrm{d}[\ell n(\sigma)] + \mathrm{d}[\ell n(A)]\} + \frac{\eta K}{Z}\mathrm{d}[\ell n(K)] + \frac{\mathrm{d}p}{\sigma Z u^2} = 0 \tag{8}$$

Using the definition of Z, the second term in Eq. (8) can be written as

$$\frac{\eta K}{Z}\mathrm{d}[\ell n(K)] = \frac{\mathrm{d}Z}{Z} = \mathrm{d}[\ell n(Z)] \tag{9}$$

Substitution of Eq. (9) into Eq. (8) results in

$$\mathrm{d}[\ell n(\sigma)] + \mathrm{d}[\ell n(A_v)] = \frac{\mathrm{d}p}{\sigma Z u^2} \tag{10}$$

where $A_v = A/Z$, the virtual area ratio. Equation (10) can also be written as

$$\mathrm{d}[\ell n(\sigma)] + \mathrm{d}[\ell n(A_v)] = a_v^2\frac{\mathrm{d}[\ell n(\sigma)]}{u^2} \tag{11}$$

where a_v is given by

$$a_v = \left[\frac{1}{Z}\frac{\mathrm{d}p}{\mathrm{d}\sigma}\right]^{1/2}$$

Equation (11) can be expressed as

$$\frac{\mathrm{d}[\ell n(\sigma)]}{\mathrm{d}[\ell n(A_v)]} = \frac{M_v^2}{1 - M_v^2} \tag{12}$$

where $M_v = u/a_v$.

Using Eq. (1), Eq. (12) can also be written as

$$\frac{\mathrm{d}[\ell n(uZ)]}{uZ} = \frac{\mathrm{d}(A_v)/A_v}{M_v^2 - 1} \tag{13}$$

Equations (12) and (13) are in the same form as available for the pure gas case or for the equilibrium gas-particle case. From the general expression for virtual speed of sound introduced in Eq. (11), the limiting speeds of sound, namely, the equilibrium and frozen cases, can easily be obtained[10] and are given by

Equilibrium case:

$$(a_e^2) = \frac{(1 + \eta\delta)}{(1 + \eta)(1 + \gamma\eta\delta)}\gamma T\frac{1}{(1 - \zeta)^2} \tag{14}$$

Frozen case:

$$(a_f^2) = \frac{\gamma T}{(1 - \zeta)^2} \tag{15}$$

Therefore, introduction of the parameters Z and A_v has served the purpose of getting a new expression for speed of sound. Moreover, hitherto not available general relations between area ratio and Mach number have been obtained for nonequilibrium gas-particle nozzle flows. The new definitions and new relations that have been derived in this section will be used in the following sections to transform the governing equations into similar form.

Transformation of Governing Equations

As discussed earlier, appropriate correlating parameters and the similar solutions are strongly desired to circumvent the cumbersome job of repeating the solution procedure. The similar solutions not only eliminate the need for repeated complex computations but also provide the experimentalist with the badly needed correlating parameters.

The reservoir conditions are normally considered for nondimensionalization of the flow variables; characteristic distance and area ratio are provided by the nozzle scale parameter L' and the nozzle throat area A'_*, respectively. The quantities in the nondimensional form are

$$T = T'/T'_0, \quad P = P'/P'_0 = P'/\{[(\gamma - 1)/2\gamma]\rho'_0 u'^2_0\}$$

$$u = u'/u'_0 = u'/(2c_p T'_0)^{0.5}, \quad A = A'/A'_*$$

$$\rho = \rho'/\rho'_0, \quad x = x'/L', \quad \tau_v = \tau'_v/(L'/u'_0)$$

The governing equations[8] of the nonequilibrium gas-particle nozzle flow can therefore be given in the nondimensionalized form (for finite volume of particles in the mixture) as follows:

Continuity (gas):

$$(1 - \zeta)\rho u A = (1 - \zeta_*)\rho_* u_* = \dot{m} \tag{16}$$

Continuity (particle):

$$\sigma_p u_p A = \zeta_* \rho_{p*} u_{p*} = \dot{m}_p = \eta \dot{m} \tag{17}$$

Momentum (mixture):

$$(1 - \zeta)\rho u \frac{du}{dx} + \eta \rho_p u_p \frac{du_p}{dx} + \frac{\gamma - 1}{2\gamma} \frac{dp}{dx} = 0 \tag{18}$$

Energy (mixture):

$$2u \frac{du}{dx} + \frac{dT}{dx} + \eta \left[2u_p \frac{du_p}{dx} + \delta \frac{dT_p}{dx} + \frac{\gamma - 1}{\gamma} \frac{1}{\rho_p} \frac{dp}{dx} \right] \tag{19}$$

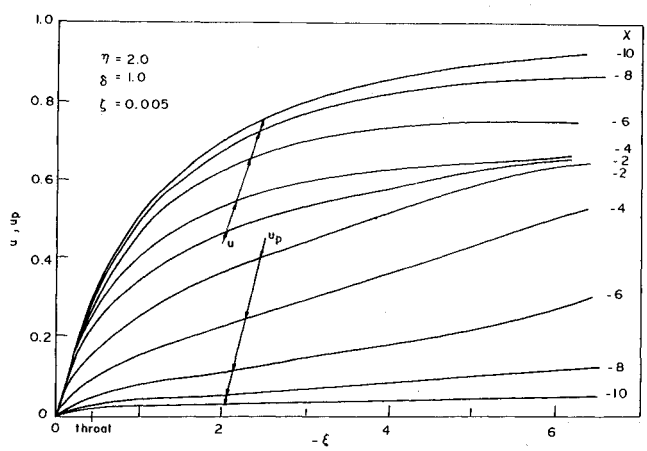

Fig. 3 Gas and particle velocity variation along the nozzle axis ($\eta = 2$, $\zeta = 0.005$).

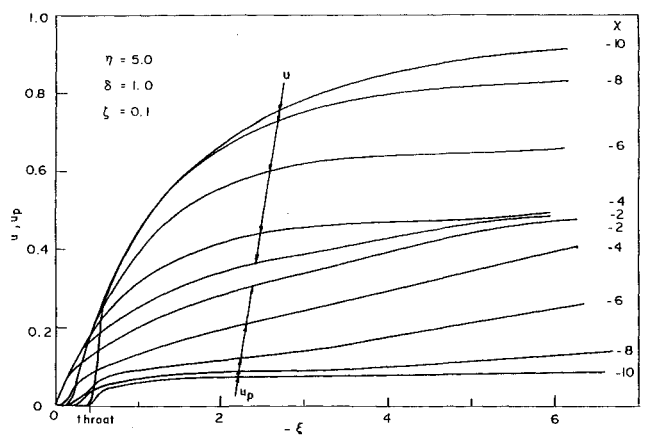

Fig. 4 Gas and particle velocity variation along the nozzle axis ($\eta = 5$, $\zeta = 0.1$).

Drag:

$$\frac{du_p}{dx} = \frac{u - u_p}{u_p} \frac{f(Re)}{\tau_{v_0}} T^{1/2} + \frac{\zeta}{\eta} \frac{du}{dx} + \zeta \frac{du_p}{dx} + C_{v_m} \frac{\rho}{\rho_p} \frac{d(u - u_p)}{d_x} \tag{20}$$

Heat transfer:

$$\frac{dT_p}{dx} = \frac{T - T_p}{u_p} \frac{Nu(Re)}{\tau_{v_0}} \frac{T^{1/2}}{2} \tag{21}$$

Equation of state:

$$p = \rho T \tag{22}$$

where C_{v_m}, the shape factor for the carried mass, is 0.5 for spherical particles, $\tau_{v_0} = \tau'_{v_0}\,(u'_0/L'_0)$, $\mu \approx T^{1/2}$, and Nu is the Nusselt number. Differentiating Eqs. (16) and (17) with respect to x and combining them results in an equation for the volume fraction of the particles:

$$\frac{d\zeta}{dx} = \zeta(1 - \zeta)\left(\frac{1}{\rho} \frac{d\rho}{dx} + \frac{1}{u} \frac{du}{dx} - \frac{1}{u_p} \frac{du_p}{dx} \right) \tag{23}$$

In Eq. (20) all of the factors that influence the particle motion like Stokes drag, pressure gradient, and virtual mass effect are considered. The concentration of the particles σ_p is defined as $\sigma_p = \zeta \rho_p$. Since ρ_p is a constant, ζ can be treated as a variable instead of σ_p, and hence an equation for ζ is presented in Eq. (23). Therefore, one of the equations (16) or (17) and Eqs. (18–23) represent seven equations for the seven unknowns: ρ, ζ, p, u, u_p, T, and T_p.

For the present analysis, a new independent variable α, defined as $\alpha = -\ell n(\sigma)$, is introduced. Using the equation of state, the term dp/dx can be eliminated from Eqs. (18) and (19), and the set of governing equations are written in the transformed form with α as the independent variable:

$$(1 - \zeta)u \frac{du}{d\alpha} + \eta(1 - \zeta)u \frac{du_p}{d\alpha} + \frac{\gamma - 1}{2\gamma} \left[\frac{dT}{d\alpha} - T \right] = 0 \tag{24}$$

$$2u \frac{du}{d\alpha} + \frac{dT}{d\alpha} + \eta \left[2u_p \frac{du_p}{d\alpha} + \delta \frac{dT_p}{d\alpha} + \frac{\gamma - 1}{\gamma} \frac{\zeta}{1 - \zeta} \frac{u_p}{u} \frac{1}{\eta} \left(\frac{dT}{d\alpha} - T \right) \right] = 0 \tag{25}$$

$$\frac{du_p}{d\alpha} = \frac{1}{\{1 - \zeta + C_{v_m}(\zeta u_p)/[u\eta(1 - \zeta)]\}} \left[\frac{u - u_p}{u_p} \times \frac{f(Re)}{N_s} T^{1/2} [Zu(1 - \zeta)]^{-1/ij} e^{\lambda + \alpha/ij} + \frac{du}{d\alpha} \frac{\zeta}{\eta} + C_{v_m} \frac{\zeta}{1 - \zeta} \frac{u_p}{u} \frac{1}{\eta} \frac{du}{d\alpha} \right] \tag{26}$$

$$\frac{dT_p}{d\alpha} = \frac{T - T_p}{u_p} \frac{1}{\delta} \frac{Nu(Re)}{2N_s} T^{1/2} [Zu(1 - \zeta)]^{-1/ij} e^{\lambda + \alpha/ij} \tag{27}$$

$$\frac{d\zeta}{d\alpha} = \zeta(1 - \zeta)\left[\frac{1}{u} \frac{du}{d\alpha} - \frac{1}{u_p} \frac{du_p}{d\alpha} - 1 \right] \tag{28}$$

where

$$N_s = \frac{M_v^2}{M_v^2 - 1} (1 - A_v^{-1/i})^{(j-1)/j}$$

$$\lambda = \ell n \left\{ \frac{[(1 - \zeta_*)(\rho_* u_*)]^{1/ij}}{ij\tau_{v_0}} \right\} \tag{29}$$

Here an expression for the term $(d\alpha/dx)$ appearing in Eqs. (20) and (21) due to this transformation has been derived using Eq. (12), and the different terms of this expression have been

grouped into N_s and λ. The parameter λ contains many of the parameters of the problem, and the equations have been transformed into a similar form. The parameters i and j govern the shape for a family of nozzles given as $A_v = (1 + x^j)^i$.

Character of Similar Equations

Equations (24–28) constitute the five transformed governing equations in similar form with u, u_p, T, T_p, and ζ as dependent variables and α as independent variable. However, these equations also contain a term N_s that is a function of A_v, M_v, and nozzle shape parameters i and j. This function has been correlated in terms of the new independent variable and is given in one of the following sections. The parametric structure of these similar equations is described as follows.

The leading and important parameter that includes almost all of the parameters of the problem is λ, and hence it is expected that the similar solutions would depend strongly on this parameter. In addition, the equations also contain the parameters (ij), δ, $f(Re)$, $Nu(Re)$, and η. Since the product (ij) appears as a single parameter in the equations, a given value of (ij) represents a family of nozzle shapes (for example, $ij = 2$ for both hyperbolic and conical nozzles). Hence, similar solutions can be obtained for a family of nozzle shapes. The parameter δ that is the ratio of specific heats of particle phase to gas phase appears separately, and hence similar solutions have to be repeated for different values of δ. However, the sensitivity of similar solutions to variation in δ values is found[10] not to be significant. The functions $f(Re)$ and $Nu(Re)$ also appear separately in the transformed governing equations. Since the Reynolds number in a gas-particle flow is based on the particle diameter that is very small in comparison with the characteristics length of the problem, the range of Reynolds number of interest in gas-particle flow rarely exceeds a few hundred. Many empirical curve fits to the standard drag coefficient can be found in the literature.[16] A good fit to the standard drag curve is reported in Ref. 17 and is given by $C_D = (24/Re)[1 + Re^{2/3}/6]$. However, expressions for these two functions corresponding to Stokes drag law have been used in the present analysis for mathematical simplification. It is shown later in this paper that the results from the present method using Stokes drag law for the drag coefficient compares to a good extent with the steady-state results obtained from time-marching numerical technique employing the Mac Cormack scheme and using the expressions for C_D given earlier. The similar equations also depend directly on η since Z is a function of η.

Initial Conditions

In the reservoir, where the flow starts, an equilibrium condition is assumed. In the equilibrium limit, since $\tau_v \to 0$, the drag and heat transfer rate equations need not be considered and only the mixture momentum and energy equations as given in Eqs. (24) and (25) need to be considered. Therefore, solving these two equations, the equilibrium solution can be obtained as

$$\alpha + \ell n(T)/(\Gamma - 1) = \text{const} \tag{30}$$

This is a relation proved[8] in the case of isentropic change of state of gas-particle mixture and the constant involved is, therefore, the reservoir entropy. Equation (30) can also be written as

$$\alpha + \ell n(T)/(\Gamma - 1) = (S_0 - S_r) \tag{31}$$

The equilibrium flow solution can be obtained from Eq. (31) with α as the independent variable and $(S_0 - S_r)$ as a parameter. It may be noted here that this solution does not depend on the nozzle shape.

Nonequilibrium Equations

To start the nonequilibrium solution procedure, the equilibrium initial conditions can now be obtained from Eq. (31). But from Eq. (31) it is apparent that the reservoir entropy has to be specified to obtain the equilibrium solution and hence $(S_0 - S_r)$ appears as an additional parameter. As mentioned earlier, the other significant parameter is λ. The two parametric dependence of the problem can then be reduced to a single parametric dependence by the following additional transformation.

A new independent variable ξ is introduced and is defined as

$$\xi = (S_0 - S_r) - \alpha \tag{32}$$

Therefore, the equilibrium entropy expression given by Eq. (31) reduces to universal form and can be given as

$$\xi = \ell n(T)/(\Gamma - 1) \tag{33}$$

The similar governing equations can then be written for the nonequilibrium case with ξ as the independent variable as

$$(1 - \zeta)u \frac{du}{d\xi} + \eta(1 - \zeta)u \frac{du_p}{d\xi} + \frac{\gamma - 1}{2\gamma}\left(\frac{dT}{d\xi} + T\right) = 0 \tag{34}$$

$$2u \frac{du}{d\xi} + \frac{dT}{d\xi} + \eta\left[2u_p \frac{du_p}{d\xi} + \delta \frac{dT_p}{d\xi} + \frac{\gamma - 1}{\gamma} \frac{\zeta}{1 - \zeta} \frac{u_p}{u} \frac{1}{\eta}\left(\frac{dT}{d\xi} + T\right)\right] = 0 \tag{35}$$

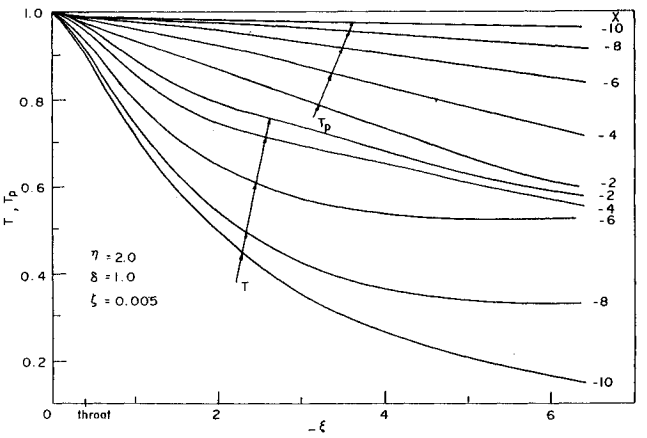

Fig. 5 Gas and particle temperature variation along the nozzle axis ($\eta = 2$, $\zeta = 0.005$).

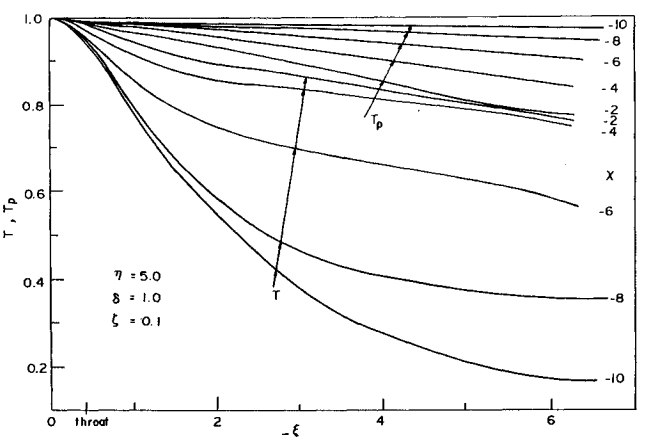

Fig. 6 Gas and particle temperature variation along the nozzle axis ($\eta = 5$, $\zeta = 0.1$).

$$\frac{du_p}{d\xi} = \frac{1}{\{1-\zeta+C_{v_m}(\zeta u_p)/[u\eta(1-\zeta)]\}}\left\{-\frac{u-u_p}{u_p}\right.$$
$$\times\frac{f(Re)}{N_s}T^{1/2}[Zu(1-\zeta)]^{-1/ij}e^{\chi-\xi/ij}$$
$$\left.+\frac{du}{d\xi}\frac{\zeta}{\eta}+C_{v_m}\frac{\zeta}{1-\zeta}\frac{u_p}{u}\frac{1}{\eta}\frac{du}{d\xi}\right\} \quad (36)$$

$$\frac{dT_p}{d\xi} = -\frac{T-T_p}{u_p}\frac{1}{\delta}\frac{Nu(Re)}{2N_s}T^{1/2}[Zu(1-\zeta)]^{-1/ij}e^{\chi-\xi/ij} \quad (37)$$

$$\frac{d\zeta}{d\xi} = \zeta(1-\zeta)\left(\frac{1}{u}\frac{du}{d\xi}-\frac{1}{u_p}\frac{du_p}{d\xi}+1\right) \quad (38)$$

where $\chi = \lambda + (S_0 - S_r)/(ij)$. The equations have thus been transformed into a similar form, and a general correlating parameter χ has been obtained. This parameter, which is given later in dimensional form, combines many of the parameters of the problem and would mainly control the behavior of the similar solutions. It can also be inferred that smaller χ corresponds to larger particles and larger χ corresponds to smaller particles. Furthermore, the function N_s has been correlated in terms of the parameter ξ.

The function N_s is given by

$$N_s = \frac{M_v^2}{M_v^2-1}(1-A_v^{-1/i})^{(j-1)/j} \quad (39)$$

The effect of various reservoir conditions and particle characteristics on this function has been shown[10] to be insignificant, and a single correlation for variation of N_s along the nozzle length has been obtained. A curve fit to the average

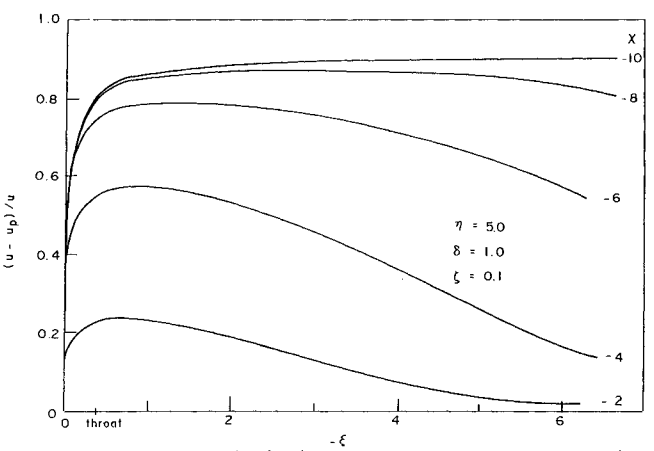

Fig. 7 Velocity lag $(u-u_p)/u$ along the nozzle axis.

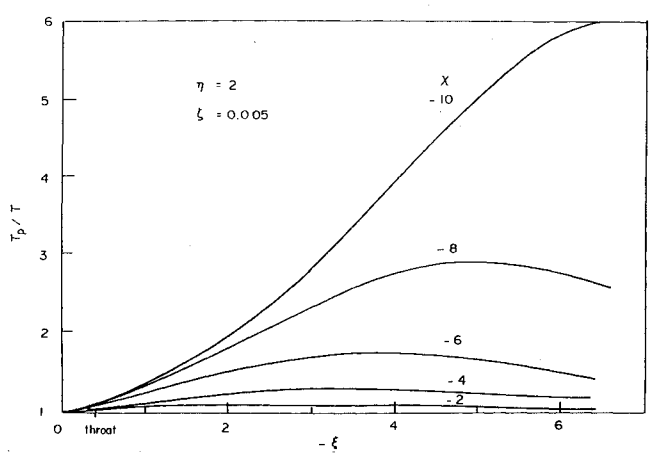

Fig. 8 Temperature lag (T_p/T) along the nozzle axis.

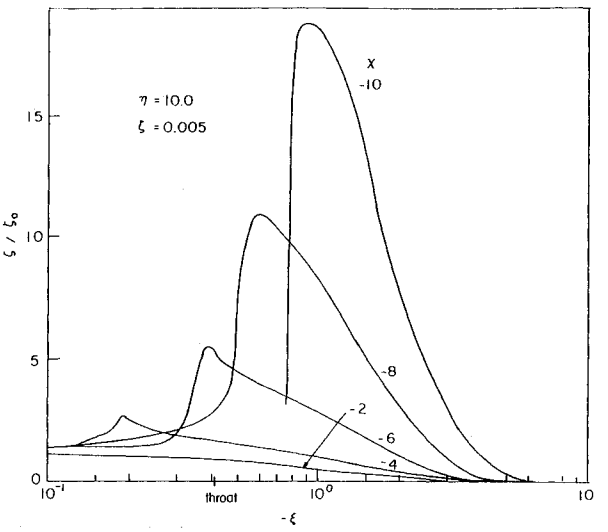

Fig. 9 Particle volume fraction variation along the nozzle axis ($\eta = 10$, $\zeta = 0.005$).

curve shown in Fig. 1 is made and is represented by a simple analytical expression of the form given as follows:

$$\begin{aligned}
N_s &= 0.09 - 35[0.99 - \xi_*/\xi]^{1.48} \\
&\qquad \text{if} \quad 0.973 < \xi_*/\xi \le 0.985 \\
&= 4.32 - 2.6[\xi_*/\xi - 0.96]^{-0.11} \\
&\qquad \text{if} \quad 0.985 < \xi_*/\xi \le 1.01 \\
&= 4.38 - 2.7[\xi_*/\xi - 0.96]^{-0.11} \\
&\qquad \text{if} \quad 1.01 < \xi_*/\xi \le 1.06 \\
&= 4.38 - 2.7[\xi_*/\xi - 0.98]^{-0.11} \\
&\qquad \text{if} \quad 1.08 < \xi_*/\xi \le 1.16 \\
&= 1.06 \\
&\qquad \text{if} \quad \xi_*/\xi > 1.16
\end{aligned} \quad (40)$$

The variation of N_s along the nozzle length can be obtained using these fitted expressions. This correlation for N_s is used in obtaining similar solutions.

Results and Discussions

Equations (34–38) for the nonequilibrium gas-particle nozzle flows were solved using the Runge-Kutta-Gill method. The starting value of χ is selected in such a way that the flow remained near equilibrium in the nozzle reservoir for different values of ζ and η. Apart from the special problem in starting the integration from an initial equilibrium state, it may be noted that the usual numerical methods, such as the fourth-order Runge-Kutta-Gill method, generally encounter a serious instability problem for near-equilibrium flow conditions. To maintain stability near equilibrium, the integration step size must be kept very small. Thus the overall computing time may become excessively large if an appreciable region of near-equilibrium flow is involved. This is the reason quoted in earlier analyses[18–20] as to why computation has not been carried out for very small particles in submicron ranges (which cope with the gas expansion process and the flow tends to be in equilibrium condition) for which the equations become stiff. Fortunately, specification of the particle diameter d_p' is not required in the current investigation.

Since the particle volume fraction ζ itself is a variable, the equations are solved for different initial values of ζ. The variation in the initial values of ζ implies that the particle material density ρ_p' is also varied since $\eta = [\zeta\rho_p' u_p]/[(1-\zeta)\rho' u']$, and therefore $(\rho'/\rho_p') = \{\zeta/[(1-\zeta)\eta]\}$ in the reservoir since $u' = u_p'$. Typical values of (ρ'/ρ_p') are given by the limits 0.0001 and 0.05.

From expression (13), it can easily be inferred that the virtual Mach number M_v reaches unity where the virtual area

ratio A_v becomes minimum. The verification of this property has been carried out, and variations of A, A_v, and M_v are shown in Fig. 2. The location of virtual Mach number equal to unity as well as the location of minimum virtual area ratio A_v do coincide.

A set of similar solutions for different values of ζ and η are shown in Figs. 3–6 for different loading ratios and $ij = 2.0$. The transformed set of governing equations contain only the product factor (ij). But the function N_s contains i and j separately and has been correlated to get a single expression independent of i and j. Therefore, specification of the values of the parameters i and j explicitly is not required.

From the velocity and temperature curves (Figs. 3–6), it is clear that the particles always lag behind the gas during the expansion process. As the loading ratio η of the particles in the mixture is increased, more energy will have to be spent by the gas in dragging the particles out, and hence the gas velocity for larger η is expected to be less than that for smaller η for a given χ and ζ. This can be observed from Figs. 3–6. Another interesting inference from these figures on the flow behavior at different χ is presented later in this section.

The variation of the lag of the particles defined as $[(u - u_p)/u]$ along the nozzle length for different values of the parameter χ is shown in Fig. 7. For all values of χ, the lag increases rather suddenly from almost negligible value at the reservoir and reaches a maximum near the nozzle throat and then decreases far downstream. This decrease in the lag is significant at higher values of χ (near equilibrium flow). For smaller values of χ, the lag is almost constant along the entire nozzle length. This is expected since the particles freeze for smaller values of χ. The particle to gas temperature ratio T_p/T variation along the nozzle length for different values of χ is shown in Fig. 8. Similar observations made for velocity lag can be inferred from this figure too.

Figures 9 and 10 show the variation of the particle volume fraction along the nozzle length. It is clear from these figures that the volume fraction increases along the nozzle axis, reaches a peak, and then decreases. At a smaller cross section, the volume occupied by the particles increases, or in other words the volume fraction of the particles at smaller cross sections increases. One more observation from these figures is that the peaking of the particle volume fraction is shifted downstream as the value of χ is decreased. In other words, for smaller value of χ, which corresponds to larger particles, the particles are frozen and hence are not affected by the expansion process until there is a drastic change in the flow characteristics immediately after the nozzle throat. Consequently, the volume fraction reaches a maximum value in the downstream portion of the nozzle. As evident from the figures, the location of the peak value of volume fraction moves downstream from the nozzle throat as the value of χ decreases (i.e., the flow tends towards frozen condition). The volume fraction not only gets affected by the gas velocity variation but also by the fast changing gas density. After the peak, the volume

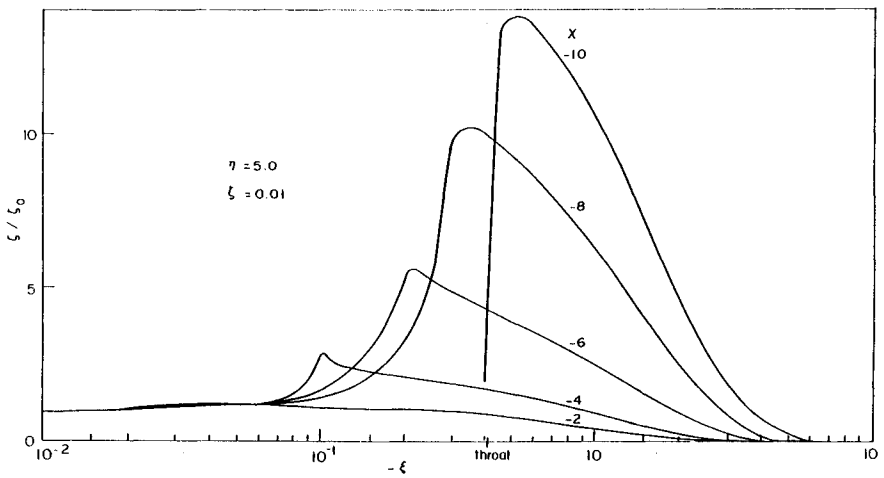

Fig. 10 Particle volume fraction variation along the nozzle axis ($\eta = 5$, $\zeta = 0.01$).

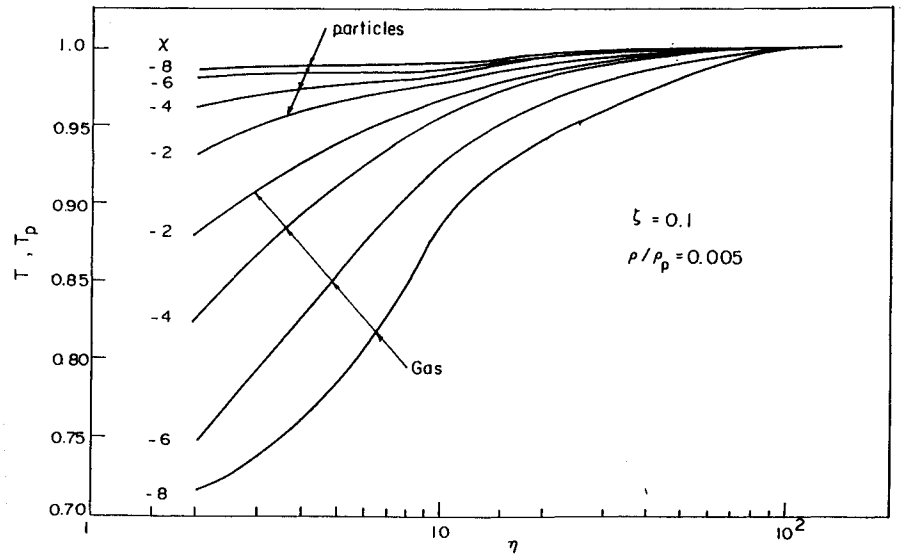

Fig. 11 Approach to isothermality of the gas and particle temperatures at large loading ratios of particles in the mixture.

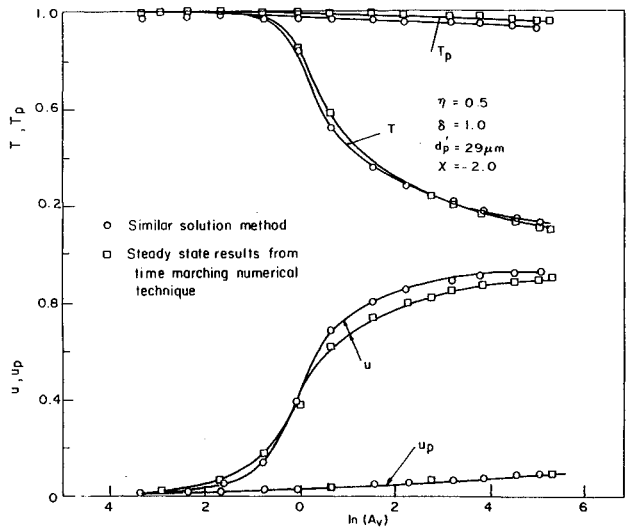

Fig. 12 Comparison of similar solutions with steady-state results of time-marching numerical technique.

fraction decreases significantly along the nozzle length. This is understandable since the large decrease in density of the gas in the nozzle downstream of the throat affects the particles significantly.

At the nozzle throat another interesting phenomenon can be observed from the similar solutions. Figure 11 shows the gas and particle temperatures at the throat, plotted as a function of loading ratio for different χ values at $\rho'/\rho_p' = 0.005$. The phenomenon here is that both the gas and particle temperatures approach the reservoir temperature for higher loading ratios. This is exactly similar to the one observed in Ref. 11, assuming constant fractional lag of the particles. This phenomenon further substantiates the similar solution results for the nonequilibrium gas-particle nozzle flows. In other words, the tendency of the flow to become isothermal at larger loading ratios is proved with no assumption regarding lag of the particles.

The similar solution results can easily be transformed into the physical plane using the definition of ξ. To compare the results obtained from similar solution method, computations have been carried out for obtaining steady-state results from a time-marching numerical technique (briefly described in the Appendix) employing the standard Mac Cormack predictor-corrector scheme. The results from both the methods are presented in Fig. 12 for typical parametric conditions. Similar solution results compare to a good extent (i.e., within 2-3% variation) with the steady-state results except for a short length downstream of the nozzle throat as shown in this figure.

As evident from similar solutions presented earlier, the parameter χ largely controls the characteristics of the similar solutions. This parameter includes several important physical parameters of the problem, and its characteristics are discussed here. The expression χ is given in dimensional form by

$$\chi = \ell_n\left\{\frac{[(1-\zeta_*)(\rho_* u_*)]^{1/ij} L' 18\mu_0'}{iju_0'\rho_p'(d_p')^2}\right\} + (S_0' - S_r')/[R(ij)] \quad (41)$$

From Eq. (41) it is apparent that χ contains all of the important parameters like reservoir conditions, nozzle throat height and expansion angle, nozzle shape factor (ij), and particle relaxation time τ_v'. From this, a relation between the diameter of the particles d_p' and the parameter χ can be obtained. Therefore, as mentioned earlier, specification of the particle diameter d_p' is not required in the current investigation. Hence, by changing other parameters in the expression for χ, different particle diameters can be obtained for a given value of χ.

Particle diameters for different parameters for χ can be calculated, and it can be inferred from these calculations that larger values of χ correspond to smaller diameter particles and smaller values of χ correspond to larger diameter particles. From similar solution results given in Figs. 3-6 it is clear that, for larger values of χ, particle velocities and temperatures try to cope with the expansion process of the gas and hence the flow tends toward a near-equilibrium condition. For smaller values of χ, it is clear from these figures that the particles respond to the expansion process very slowly. In other words, the particle properties are almost frozen for smaller values of χ. Therefore, variation in the value of χ scans the flow from near-equilibrium to near-frozen conditions, and hence the entire nonequilibrium flow solution could be presented in a single figure for a given loading ratio.

Conclusions

Through the introduction of modified definitions for speed of sound and Mach number called virtual speed of sound and virtual Mach number, simple Mach number-area ratio relations have been obtained that are applicable to the nonequilibrium gas-particle nozzle flow. They are very similar to those already existing for the pure gas case or for the equilibrium gas-particle case. The limiting (equilibrium and frozen) speeds of sound are derivable from the modified definitions. The governing equations are transformed into a similar form, and the similar solutions presented in this study represent the gas-particle nozzle flow phenomena in an exhaustive manner at different reservoir conditions, at a wide range of particle dimensions and loading ratios, and for different volume fractions of the particles as well. The cumbersome job of repeating the solution procedure for different given initial conditions could thus be obviated. The size of the particles and the loading ratio play important roles in the nozzle expansion process. It is shown that different values for the general correlating parameter represents the complete spectrum of the nonequilibrium nozzle flow from near-equilibrium to near-frozen regimes.

Appendix

In the time-marching numerical technique, the solution to the unsteady form of the governing equations[8] of gas-particle nozzle flow are advanced in time from an assumed initial spatial distribution of the flow variables. The marching in the intervals of time follows an iterative scheme, details of which are available in Refs. 21 and 22, and continues until the solution satisfies certain convergency conditions depending on the problem. Mac Cormack's[23] predictor-corrector scheme is used in the present study, and the spatial derivatives are expressed in forward and backward difference form for the predictor and corrector steps, respectively, since the governing equations contain only first derivatives. The integration time step is obtained from the Courant-Friedrichs-Lewy stability criterion with a multiplying factor of 0.8. The important process in the present study is the relaxation of the particle properties that are slow in comparison with the gas properties. Hence, particle velocity is used for the convergency criterion of the numerical procedure and the condition at the nth time step is given by

$$\left|\frac{u_p^n - u_p^{n-1}}{u_p^n}\right| \leq 1 \times 10^{-3}$$

From the present numerical experiment it is observed that for a given loading ratio and the particle diameter $d_p \geq 2$ μm there was no difficulty in the computational process. For particle diameters much smaller than 2 μm, a stiffness problem is encountered. In the present work, computations have been carried out for particle diameters larger than 2 μm, and one such case is presented in Fig. 12 along with similar solution results.

Acknowledgment

The first author acknowledges gratefully the Council of Scientific and Industrial Research, Government of India, for the financial support made available to him by the award of Senior Research Fellowship in Engineering.

References

[1]Marble, F. E., "Dynamics of a Gas Containing Small Solid Particles," *Fifth AGARD Combustion and Propulsion Colloquia,* Pergamon Press, Oxford, England, UK, 1963, pp. 175–214.

[2]Rudinger, G., and Chang, A., "Analysis of Non-Steady Two-Phase Flow," *Physics of Fluids,* Vol. 7, No. 11, 1964, pp. 1747–1754.

[3]Ishii, R., "Non-Equilibrium Nozzle Flows of Gas-Particles Mixtures," *Transactions of the Japanese Society of Aeronautics and Space Sciences,* Vol. 18, No. 39, 1975, pp. 29–40.

[4]Chang, I. S., "Three Dimensional Two-Phase Supersonic Nozzle Flows," *AIAA Journal,* Vol. 21, No. 5, 1983, pp. 671–678.

[5]Ishii, R., Umeda, Y., and Kawasaki, K., "Nozzle Flows of Gas-Particle Mixtures," *Physics of Fluids,* Vol. 30, No. 3, 1987, pp. 752–760.

[6]Hayashi, A. K., Matsuda, M., Fujiwara, T., and Arashi, K., "Numerical Simulation of Gas-Solid Two-Phase Nozzle and Jet Flows," AIAA Paper 88-2627, 1988.

[7]Bilicki, Z., and Kestin, J., "Physical Aspects of the Relaxation Model in Two-Phase Flow," *Proceedings of the Royal Society of London, Series A: Mathematical and Physical Sciences,* Vol. 428, 1990, pp. 379–397.

[8]Rudinger, G., "Fundamentals of Gas-Particle Flows," *Handbook of Powder Technology,* edited by J. C. Williams and T. Allen, Vol. 2, Elsevier, Amsterdam, The Netherlands, 1980.

[9]Pai, S. I., *Two-Phase Flows,* Vieweg Tracts in Pure and Applied Physics, Vol. 3, Vieweg, Braunschweig, Germany, 1977.

[10]Thulasiram, R. K., "Similar Solutions and General Correlating Parameters in Non-Equilibrium Gas-Particle Nozzle Flows," Ph.D. Thesis, Indian Inst. of Science, Bangalore, India, March 1990.

[11]Rudinger, G., "Gas-Particle Flow in Convergent Nozzles at High Loading Ratios," *AIAA Journal,* Vol. 8, No. 7, 1970, pp. 1288–1294.

[12]Rudinger, G., "Some Effects of Finite Particle Volume on the Dynamics of Gas-Particle Mixtures," *AIAA Journal,* Vol. 3, No. 7, 1965, pp. 1211–1222.

[13]Reddy, N. M., and Daum, F. L., "Similar Solutions in Vibrational Non-Equilibrium Nozzle Flows," *AIAA Journal,* Vol. 9, No. 8, 1971, pp. 1622–1624.

[14]Thulasiram, R. K., Reddy, K. P. J., and Reddy, N. M., "Theorerical Study of Optimum Performance of a Two-Phase Flow CO_2 Gasdynamic Laser," *Applied Physics Letters,* Vol. 50, No. 13, 1987, pp. 189–191.

[15]Reddy, N. M., and Thulasiram, R. K., "Transformation of Two-Phase Flow Equations into Pure Gas Type by Introducing Virtual Area Ratio and Virtual Mach Number," CP 208, American Institute of Physics, New York, July 1989, pp. 732–737.

[16]Boothroyd, R. G., *Flowing Gas-Solid Suspensions,* Chapman and Hall, London, England, UK, 1971.

[17]Fuchs, N. A., *The Mechanics of Aerosols,* Macmillan, New York, 1964.

[18]Bailey, W. S., Nilson, E. N., Serra, R. A., and Zupnik, T. F., "Gas-Particle Flow in an Axisymmetric Nozzle," *ARS Journal,* Vol. 31, No. 6, 1961, pp. 793–798.

[19]Carlson, D. J., "Experimental Determination of Thermal Lag in Gas-Particle Nozzle Flows," *ARS Journal,* Vol. 32, No. 7, 1962, pp. 1107–1109.

[20]Doi, T., "Gas-Particle Nozzle Flows and Optimum Nozzle Shape," Inst. of Space and Astronautical Sciences, Rept. 596, Tokyo, Japan, Nov. 1981.

[21]Anderson, J. D., Jr., *Modern Compressible Flow: With Historical Perspective,* McGraw-Hill, New York, 1990.

[22]Anderson, J. D., Jr., *Gasdynamic Lasers: An Introduction,* Academic, New York, 1976.

[23]Mac Cormack, R. W., "The Effect of Viscosity in Hypervelocity Impact Cratering," AIAA Paper 69-354, April 1969.